Extrapolating Species Abundance Across Spatial Scales

William E. Kunin

The analysis, measurement, and management of species abundance is central to ecology and conservation biology, but it has proved difficult to find a single index that adequately reflects the commonness or rarity of species across a range of spatial scales. Here, a scale-independent measure of species abundance is developed, using presence-absence maps at varying spatial resolutions. By extrapolating such "scale-area" curves, species abundance can be estimated accurately even at scales finer than those used to parameterize the model, a task that had previously been deemed impossible in principle.

The measurement of the abundance or rarity of species is a central problem facing the study and management of biodiversity (*1*). Rarity is complex and multidimensional; species differ in the density of their local populations, in the ubiquity of their populations across a landscape, in the geographical ranges across which they are distributed, and in many other respects (*2*). This has lead to a plethora of terms and indices; I will use the term "abundance" for the commonness or rarity of species as measured by any such index. The various aspects of abundance are often correlated with one another (*1, 3*), but they are not interchangeable, making it difficult to compare information gathered in different ways or to select appropriate conservation priorities. A method for translating abundance information between different measures is badly needed.

To attempt such a translation, the various indices must first be reduced to a common currency. This can be achieved using a commonly available device: the distributional "dotmap," in which all known occurrences of a species are plotted on a geographical grid. Existing maps of this type vary greatly in their spatial resolution, reflecting differences in survey area, data availability, and printing quality (*4*). Yet these arbitrary differences can prove important: maps of different spatial resolutions reflect different aspects of abundance (Fig. 1B). Occupied cells of very coarse grids merge to form range maps, whereas finer grids progressively reveal broad-scale habitat distributions, regional ubiquity, and local population patterns. Extremely fine grids could even be used to estimate population size (with cells roughly the size of an individual) or area covered (with still finer cells acting as pixels in a digital scanner).

This property of distributional grid maps makes them extremely useful as an analytical tool. The area deemed to be occupied on such maps (the total area of all occupied cells at scale x, which I will abbreviate A_x) can serve as the required common currency for abundance measures. This allows information from a wide range of spatial scales to be combined by plotting A_x as a function of the scale of the analysis (the area of each cell, x) on logarithmic axes (for example, Fig. 1A). Such "scale-area" curves are quite similar to the logarithmic plots used in fractal analyses of species distributions (*5*); indeed, where distributions are approximately fractal, scale-area curves should be approximately linear, with a slope of $1 - D_b/2$ [where D_b is the "box-counting" dimension of the distribution (*6*)]. Just as the fractal dimension measures the propensity of a pattern to fill space, the slope of a scale-area curve measures the degree to which a species' population fills its geographical range: the steeper the slope, the sparser the distribution. The slope and height (the intercept at an arbitrary baseline scale of, for example, 1 km^2) of a linear scale-area curve should encapsulate species abundance information across a broad range of spatial scales, providing a scale-independent description of abundance.

The fact that many abundance measures can be captured on grid maps has a second important implication: the challenge of converting between different abundance measures can be reduced to the simpler issue of translating presence-absence maps across scales. Translations from fine-scale maps to coarser scales are simple; any coarse-scale grid cell containing at least one occupied cell on the finer scale is deemed to be occupied. A coarse-scale map, however, contains less information than a fine-scale map of the same area, and so precise maps at fine resolutions cannot be generated from coarse-scale information alone. Nonetheless, scale-area curves can be used to estimate some attributes of fine-scale distributions from coarse-scale data.

To do so, some form of crude scale-area curve must be generated from the available data. A rudimentary scale-area curve can be constructed using data from as few as two scales of analysis, or even from a single distribution map at an arbitrary scale of resolution, because a coarser scale map can easily be drawn from it. The resulting scale-area curves can then be extrapolated down to finer scales, allowing abundance to be predicted at scales finer than those used to generate the

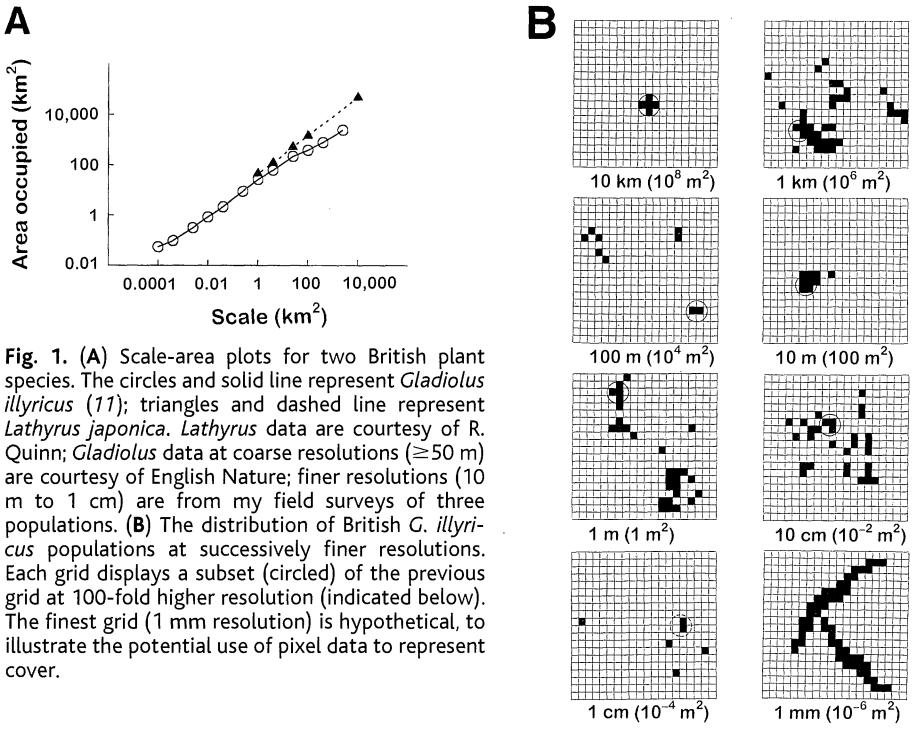

Fig. 1. (**A**) Scale-area plots for two British plant species. The circles and solid line represent *Gladiolus illyricus* (*11*); triangles and dashed line represent *Lathyrus japonica*. *Lathyrus* data are courtesy of R. Quinn; *Gladiolus* data at coarse resolutions (≥50 m) are courtesy of English Nature; finer resolutions (10 m to 1 cm) are from my field surveys of three populations. (**B**) The distribution of British *G. illyricus* populations at successively finer resolutions. Each grid displays a subset (circled) of the previous grid at 100-fold higher resolution (indicated below). The finest grid (1 mm resolution) is hypothetical, to illustrate the potential use of pixel data to represent cover.

Centre for Biodiversity and Conservation, School of Biology, University of Leeds, Leeds, LS2 9JT, UK. E-mail: w.e.kunin@leeds.ac.uk

prediction. I have tested this technique by examining distributional data for 73 species of scarce British plants for which distributional data have been published at 10 km by 10 km (100 km^2) and 2 km by 2 km (4 km^2) scales (*7*). How accurately can the finer scale abundance values be predicted from the coarser scale data alone?

I base my analyses on published 100 km^2 ("moderate") resolution maps, from which 2500 km^2 ("coarse") resolution maps were generated by superimposing a 50 km by 50 km grid. These defined a scale-area line which was then extrapolated to predict abundance for each species at a 4 km^2 ("fine") scale of analysis (*8*); the resulting predictions were than compared to published ("observed") figures for each species. There was a tight relationship between predicted and observed abundance (Fig. 2; least squared regression: observed = 0.51 + 0.866 * predicted; $F = 379.96$, $R^2 = 0.840$), but it did not correspond very closely to the predicted 1:1 relationship [regression versus prediction: $F = 50.74$, $P < 0.0001$; fraction of variance explained by the predicted line = 0.617 (*9*)]. The observed values were generally lower than expected; only 13 of the 73 observed values are at or above the predicted value (binomial probability = 2.31×10^{-8}). Thus, the scale-area curves tended to increase in slope slightly at finer scales, suggesting either that there was systematic undersampling (by about 25%) at fine scale, or else that the distributions of the plants studied were not precisely fractal over the scales considered. Species differed consistently in the slopes of their scale-area curves across scales; species with relatively steep slopes between moderate and coarse scales also displayed steep slopes between fine and moderate scales (correlation r = 0.681, $P = 3.44 \times 10^{-11}$).

If plant distributions do not appear to be strictly fractal, they nonetheless seem to depart from the predicted linear pattern in a characteristic fashion. With the accumulation of large datasets, it may become possible to develop statistical expectations as to the shape of scale-area curves. To test the notion, I divided the dataset in half and performed a linear regression on one subset (of 37 species) to estimate the area occupied at fine scale as a function of moderate- and coarse-scale areas. This relationship was then used to predict fine-scale abundance in the second subset (of 36 species). The initial subsample produced a highly significant regression model [$\log(A_f) = -1.044 + 1.598 * \log(A_m) - 0.613 * \log(A_c)$; $R^2 = 0.811$]. This model proved an accurate predictor of actual 4 km^2 occupancy in the remaining species subset (fraction of variance explained by the prediction = 0.862).

The inclusion of coarse-scale data in this model significantly improves its predictive power; if predictions are made on the basis of moderate (100 km^2) scale data alone, the fraction of the variance explained drops to 0.701—more than doubling the unexplained variation. More generally, the predictive power of the various approaches can be compared by a series of "leave-one-out" regressions, in which the fine-scale value for each species in the dataset is estimated using a regression based on all of the other species. The coarse-scale factor makes a significant contribution to these predictions ($t = -7.9$, $P < 0.00001$); its inclusion drops the cross-validated mean-squared error of the predictions from 0.112 (with moderate-scale information alone) to 0.059. The mean-squared error of the original (linear extrapolation) predictions is worse, at 0.149, but much of this is due to the apparent bias; removing this, the remaining variance is only 0.071, which is not much worse than that of the full regression model (0.065).

In both the original (linear extrapolation) analysis and the later (regression-based) one, the predicted effect of coarse-scale (2500 km^2) abundance on fine-scale (4 km^2) abundance was negative once the positive effect of moderate-scale (100 km^2) values was accounted for. This occurs despite the fact that the area occupied on fine- and coarse-scale grids are positively correlated ($r = 0.336$). The negative relationship is a consequence of interspecific differences in scale-area curve slopes; if two species have comparable abundance levels at some moderate spatial scale, the one with the steeper scale-area curve should have both a higher coarse-scale abundance and a lower fine-scale value than its fellow. This is precisely what occurred; of 21 species pairs in the dataset with identical or similar (within 2%) 100 km^2 scale abundance values, the species with the higher coarse-scale abundance had the lower fine-scale abundance in 18 cases (one-tailed binomial probability = 0.000745). The three exceptions were species with relatively similar coarse-scale values; indeed, the more dissimilar a pair's abundances were at the coarse scale, the more dissimilar (in the opposite direction) they tended to be at fine scales ($r =$

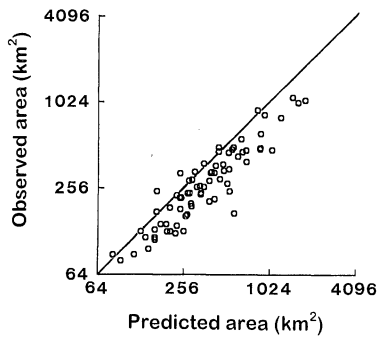

Fig. 2. Predicted and observed abundance of scarce British plant species, expressed as area occupied at a 4-km^2 scale of analysis. Predictions are based on linear extrapolation of rudimentary scale-area curves derived from data at a resolution of 100 and 2500 km^2. The diagonal line corresponds to observed = predicted.

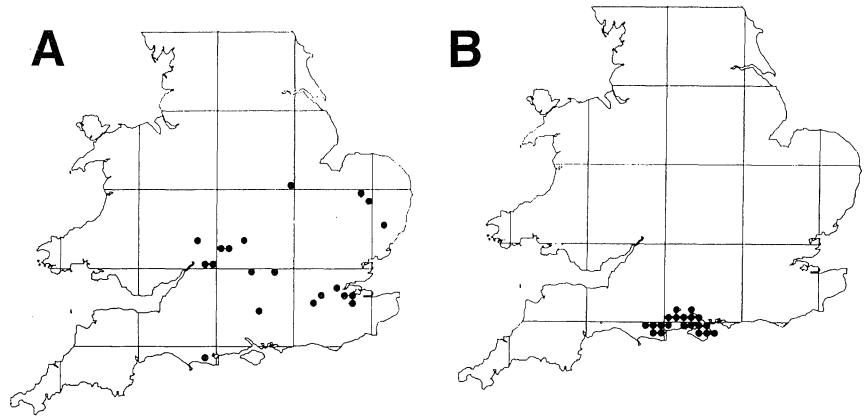

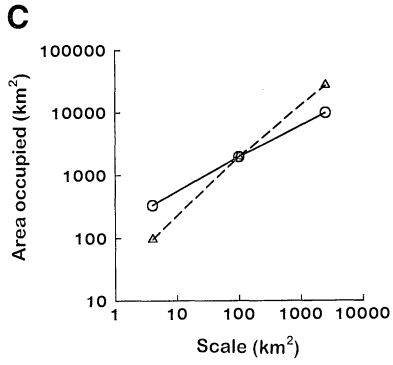

Fig. 3. British distributions of two plant species: (**A**) *Vulpia unilateralis* and (**B**) *Pulmonaria longifolia* at 100-km^2 resolution [from (*7*), adapted and reproduced with permission]. Only post-1970 records are shown. (**C**) The contrasting aggregation patterns of the two species are reflected in the slopes of their scale-area curves, with triangles and dashed lines representing *V. unilateralis* and circles and solid lines representing *P. longifolia*. Note that even though the two species are equally common at the moderate resolution shown here, they differ markedly at other scales. Extrapolating the scale-area curves suggests that *P. longifolia* may be very much commoner than *V. unilateralis* at still finer scales.

-0.574, $P = 0.00655$). The point can be expressed in less abstract terms: where occupied cells at a coarse scale occur in dense clusters, each cell is likely to include a relatively large number of populations or occurrences at finer scales, but where coarse-scale cells are sparsely scattered, each is likely to contain only one or a very few finer scale records (Fig. 3).

Scale-area curves may provide a useful descriptive and predictive tool in the study and management of species abundance. Current conservation prioritization schemes often rely on arbitrary scales of analysis; British red data lists, for example, are based on abundance measured at a 100-km^2 scale, but the ranking of species could be quite different if they were analyzed at a different scale (*10*). The use of scale-area curves (or parameters fit to them) would allow more robust prioritization and would permit explicit consideration of different forms of rarity (*2*) in conservation decision-making. Furthermore, if the patterns documented here hold across a wider range of species and scales, it may be possible to extrapolate these curves to estimate abundance at scales that would otherwise be difficult or impossible to study.

References and Notes

1. K. J. Gaston, *Rarity* (Chapman & Hall, London, 1994).
2. D. Rabinowitz, in *The Biological Aspects of Rare Plant Conservation*, H. Synge, Ed. (Wiley, Chichester, 1981), pp. 205–217; P. L. Fiedler and J. J. Ahouse, in *Conservation Biology: The Theory and Practice of Nature Conservation, Preservation, and Management*, P. L. Fiedler and S. K. Jain, Eds. (Chapman & Hall, New York, 1992), pp. 23–47.
3. K. J. Gaston, T. M. Blackburn, J. H. Lawton, *J. Anim. Ecol.* **66**, 579 (1997).
4. J. Jalas and J. Suominen, Eds., *Atlas Florae Europaeae* (Cambridge Univ. Press, Cambridge, 1988); F. H. Perring and S. M. Walters, Eds., *Atlas of the British Flora* (EP Publishing, Wakefield, UK, 1976); E. Crackles, *Flora of the East Riding of Yorkshire* (Hull Univ. Press, Hull, UK, 1990).
5. C. Loehle, *Landscape Ecol.* **5**, 39 (1990); G. Sugihara and R. M. May, *Trends Ecol. Evol.* **5**, 79 (1990); M. H. Williamson and J. H. Lawton, in *Habitat Structure: The Physical Arrangement of Objects in Space*, S. S. Bell, E. O. McCoy, H. R. Mushinsky, Eds. (Chapman & Hall, London, 1991), pp. 69–86; M. W. Palmer, *Am. Nat.* **139**, 375 (1992); H. M. Hastings and G. Sugihara, *Fractals: A User's Guide for the Natural Sciences* (Oxford Univ. Press, Oxford, 1993); R. Virkkala, *Oikos* **67**, 218 (1993); A. O. Gautestad and I. Mysterud, *ibid.* **69**, 154 (1994); B. A. Maurer, *Geographical Population Analysis: Tools for the Analysis of Biodiversity* (Blackwell, London, 1994).
6. H.-O. Peitgen, H. Jürgens, D. Saupe, *Chaos and Fractals: New Frontiers of Science* (Springer-Verlag, New York, 1992).
7. A. Stewart, D. A. Pearman, C. D. Preston, Eds., *Scarce Plants in Britain* (Joint Nature Conservation Committee, Peterborough, UK, 1994).
8. If the log area occupied at "coarse" (2500 km^2), "moderate" (100 km^2), and "fine" (4 km^2) scales are represented as A_c, A_m, and A_f, respectively, and if both scale transitions are equal in magnitude (in this case, 25-fold), the predicted fine-scale value with a linear scale-area curve can be expressed as: $A_F = 2A_M - A_C$.
9. The computation of probabilities is complicated by inbuilt positive relationships across scales: a species cannot occupy fewer cells or more area at a fine scale than it does at a coarse scale of analysis. Where possible, supplementary analyses have been added to permit probability estimates. The analysis of scale-area curve slopes, for example, has an in-built negative correlation (due to a shared 100-km^2 scale term that affects one slope positively and the other negatively), making the observed positive relationship and probability value conservative estimates. The accuracy of model predictions is measured throughout using a technique analogous to an R^2, but comparing observed values to predictions, rather than to lines of best fit. The fraction of variance explained is expressed as $(SSY - SSE)/SSY$, where $SSY = \Sigma(Y_i - \bar{Y})^2$, $SSE = \Sigma(Y_i - \hat{Y})^2$, and $\hat{Y}$ is the model prediction.
10. D. Pearman, *Watsonia* **21**, 231 (1997).
11. *Gladiolus illyricus* Surveys were conducted during July 1995 on four of the 82 50 m by 50 m cells recorded as occupied in the files of English Nature. *Gladiolus illyricus* populations were found in three of the cells. All individuals with two or more leaves were mapped using infrared distance measures triangulated to two fixed reference points at each site. Where individuals were within 10 cm of one another, these measurements were supplemented with nearest-neighbor distance and direction measurements.

12. *Gladiolus* field work was supported by the Centre for Population Biology, Imperial College, and benefited from the co-operation of the Forestry Commission and English Nature. I thank A. Shmida and J. Antonovics for raising the question, J. H. Lawton for raising the challenge, and G. H. Orians for inspiration. P. D. Sasieni, the Joint Nature Conservation Committee, and two anonymous referees provided invaluable assistance and advice.

2 March 1998; accepted 21 July 1998

Conversion of Neuronal Growth Cone Responses from Repulsion to Attraction by Cyclic Nucleotides

Hong-jun Song,* Guo-li Ming,* Zhigang He,* Maxime Lehmann, Lisa McKerracher, Marc Tessier-Lavigne, Mu-ming Poo†

Nerve growth is regulated by attractive and repulsive factors in the nervous system. Microscopic gradients of Collapsin-1/Semaphorin III/D (Sema III) and myelin-associated glycoprotein trigger repulsive turning responses by growth cones of cultured *Xenopus* spinal neurons; the repulsion can be converted to attraction by pharmacological activation of the guanosine 3′,5′-monophosphate (cGMP) and adenosine 3′,5′-monophosphate signaling pathways, respectively. Sema III also causes the collapse of cultured rat sensory growth cones, which can be inhibited by activation of the cGMP pathway. Thus cyclic nucleotides can regulate growth cone behaviors and may be targets for designing treatments to alleviate the inhibition of nerve regeneration by repulsive factors.

The development of specific connections between neurons and their targets is determined in part by selective pathway choices made by growing axons, which are directed by guidance factors present in the embryo (*1*). These factors may exert either attractive or repulsive action on the extension of axonal growth cones (*1, 2*). There is evidence that attractive and repulsive responses might be mechanistically related. Attractive responses to netrins, mediated by the DCC/UNC-40 family of proteins, can be converted to repulsion by coexpression of proteins of the UNC-5 family (*3*). In addition, attractive effects of brain-derived neurotrophic factor (BDNF) and netrin-1 on *Xenopus* spinal neurites in culture can be converted to repulsion by inhibition of protein kinase A activity (*4, 5*). That a conversion (rather than an inhibition) of the response can occur suggests that some of the same cytoplasmic components may be used for both attractive and repulsive responses. This also raised the question of whether the action of repulsive factors can be converted to attraction.

Collapsin-1/semaphorin III/D (Sema III), a diffusible member of the semaphorin family, can repel or cause collapse of growth cones in culture (*6*). Defects in Sema III knockout mice suggest that Sema III creates exclusion zones for axons and drives axonal fasciculation through surround repulsion (*7*). We analyzed the effect of a microscopic gradient of Sema III on growth cones of cultured *Xenopus* spinal neurons. Sema III–containing saline was applied in pulses from a micropipette positioned 100 μm from the center of the growth cone and at a 45° angle with

H-j. Song, G-l. Ming, M-m. Poo, Department of Biology, University of California at San Diego, La Jolla, CA 92093–0357, USA. Z. He and M. Tessier-Lavigne, Howard Hughes Medical Institute, Department of Anatomy and Department of Biochemistry and Biophysics, University of California at San Francisco, San Francisco, CA 94143–0452, USA. M. Lehmann and L. McKerracher, Departement de Pathologie, Université de Montreal, and McGill University, C.P. 6128, Succursale Centre-ville Montreal, Quebec H3C 3J7, Canada.

*These authors contributed equally to this work.
†To whom correspondence should be addressed. E-mail: mpoo@ucsd.edu